

b. Inlet characteristics.

(1) Tidal inlets generally have a short, narrow channel passing between two sandy barrier islands (Figure II-6-1) and connect the ocean (or sea) to a bay. Some bays are small enough (on the order of tens of kilometers or less) for the water surface to rise and fall uniformly (co-oscillate) in response to the forcing ocean tide. Larger estuaries sometimes have broader junctions with the sea and may be long enough (hundreds of kilometers) to contain nearly an entire tidal wave length, thus having a variable water level at a given instant of time throughout the bay. Most methods discussed in this chapter apply to inlets that are closer to having a co-oscillating tide, but can be applied to most inlet systems as long as the tidal period is long compared to the time required for a shallow-water wave to propagate from the inlet to the farthest point in the bay, i.e.,

$$T \gg \frac{L_b}{\sqrt{gd_b}} \quad (\text{II-6-1})$$

where L_b is the distance to the farthest point, d_b is average bay depth, and T is typically taken as 12.42 hrs \times 60 min/hr \times 60 sec/min or 44,712 sec (for locations with semidiurnal or twice daily tides) or 89,424 sec for once-daily tides.

(2) The configuration of an individual inlet can vary significantly over time. Often the configuration is highly influenced by geology or peculiarities of the site, rather than a simple equilibrium of sediment and hydrodynamics. Convergence of flows from several directions at either side of the inlet can create strong turbulence that scours the channel deeply through the narrowest part of the inlet, called the inlet gorge, and silts in the channel on the bay and ocean sides. Maximum depths generally in the range of 4-15 m may occur in such channels, whereas seaward channel depths may diminish to 1.5-3 m where the flow has diffused and wave-driven sediment transport is important. Inside the inlet, water may diverge into one or more channels among shoal areas created by the deposition of sand from the ocean beaches. The resulting bathymetry can be a complex pattern of bars, shoals, and channels. Hayes (1980) shows the ocean-side ebb-tidal delta morphology for an unstructured inlet (Figure II-6-2).

c. Inlet variables. Although inlet systems can be quite complex, for the purpose of simple hydraulic analysis, the immediate inlet region can be approximated by key parameters which, although simplified, permit an analytical treatment of its hydraulics and a useful analysis of inlet systems. Analysis by Vincent and Corson (1980, 1981) shows the range of size of a number of inlet parameters based on 67 inlets that had been subjected to little or no human intervention. Figure II-6-3 defines an oceanside channel length L_{mw} (used for their particular study, and not to be confused with channel length defined later), depth at the crest of the outer bar in the channel (DCC), and location of inlet minimum width A_{mw} . Figure II-6-4 defines the area of the ebb tidal delta, AED, bounded by the depth contour of DCC (until it parallels the shoreline), the line joining this location and the shoreline and the line across the inlet minimum width. Cross-sectional area at the minimum inlet width (A_{mw}) is plotted against channel length (L_{mw}) in Figure II-6-5, against ebb tidal delta area (AED) in Figure II-6-6, against maximum channel depth (DMX) measured at minimum width section in Figure II-6-7, and against channel-controlling depth (DCC), the minimum depth across the outer bar, in Figure II-6-8. All parameters vary in log-linear relation to A_{mw} over several orders of magnitude. The 95-percent confidence bands are also plotted. O'Brien's (1931) observed that there is a direct relationship between the inlet's minimum cross-sectional flow area A (this is the minimum area A_c , not necessarily the area at the location of the minimum width), and the tidal prism (P) filling the bay (Figure II-6-9). This relationship will aid in defining the stability of inlet channels. The tidal prism in this case is defined as the volume of water entering through the inlet on a spring tide. Detailed methods to define inlet parameters will be discussed later.

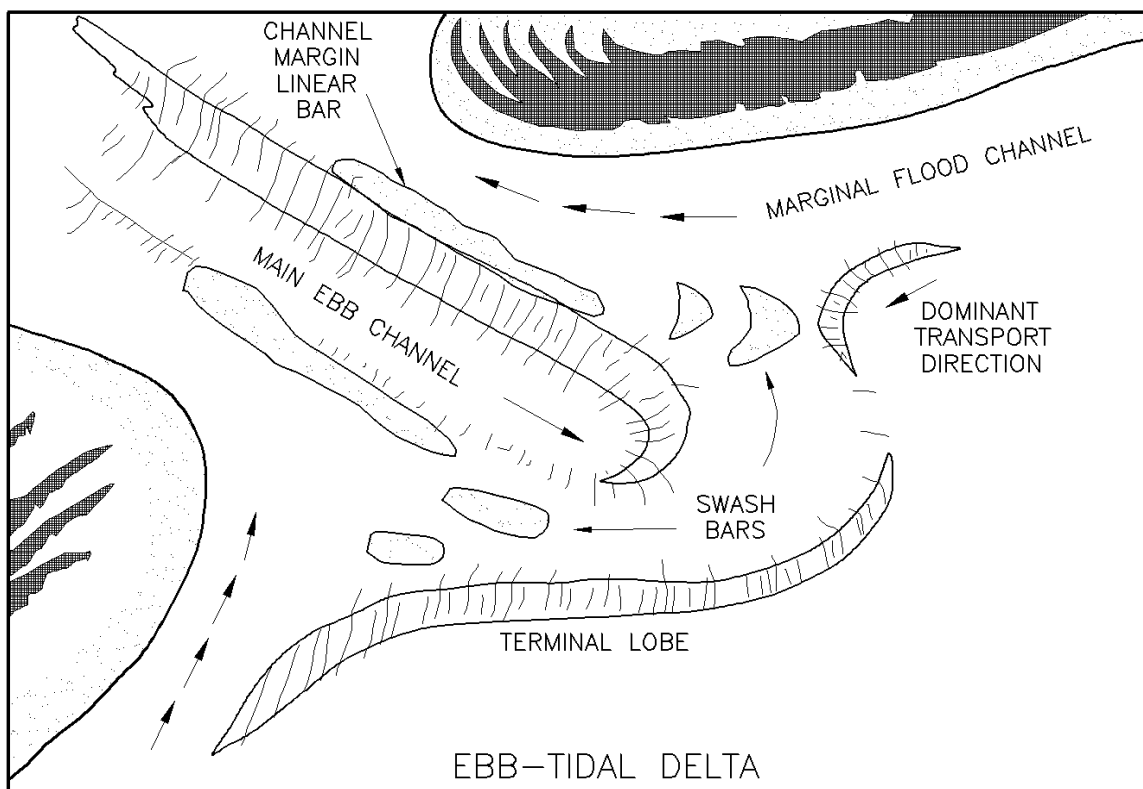


Figure II-6-2. Typical ebb-tidal delta morphology (Hayes 1980)

d. Inlet flow patterns.

(1) An inlet has a "gorge" where flows converge before they expand again on the opposite side. Shoal (shallow) areas that extend bayward and oceanward from the gorge depend on inlet hydraulics, wave conditions, and general geomorphology. All these interact to determine flow patterns in and around the inlet and locations where flow channels occur.

(2) Typical flood and ebb current patterns on the ocean side of a tidal inlet are shown in Figure II-6-10. The important aspect of this general circulation pattern is that currents usually flow toward the inlet near the shoreline (in the flood channels), even on ebb tide. The reason for this seeming paradox is the effect of wave-driven currents, (on the downdrift side of the inlet, breaking waves are turned toward the inlet due to refraction over the outer bar and on breaking, create currents toward the inlet). Further downdrift, currents are directed away from the inlet (an example of this is given in Figure II-6-11) and the effect of the ebb jet convecting or entraining ocean water as it exits the inlet creates an alongshore current at the base of the ebb jet. The "sink" flood flow pattern of the previous flood tide flow's momentum also helps sustain this flow pattern. Figure II-6-12 shows ebb and flood flow patterns from a model study of Masonboro Inlet, North Carolina, for both pre- and post-jetty conditions. Figure II-6-13 shows strength and direction of wave-generated currents plus tidal currents approaching a jetty at an inlet as measured in a physical model study. Figure II-6-14 shows the complexity of sediment flow patterns at an inlet as resolved by a field study at Essex River Inlet, Massachusetts (Smith 1991). Ebb and flood flow patterns are discussed in detail in Part II-6-2, paragraph j, *Tidal jets*.

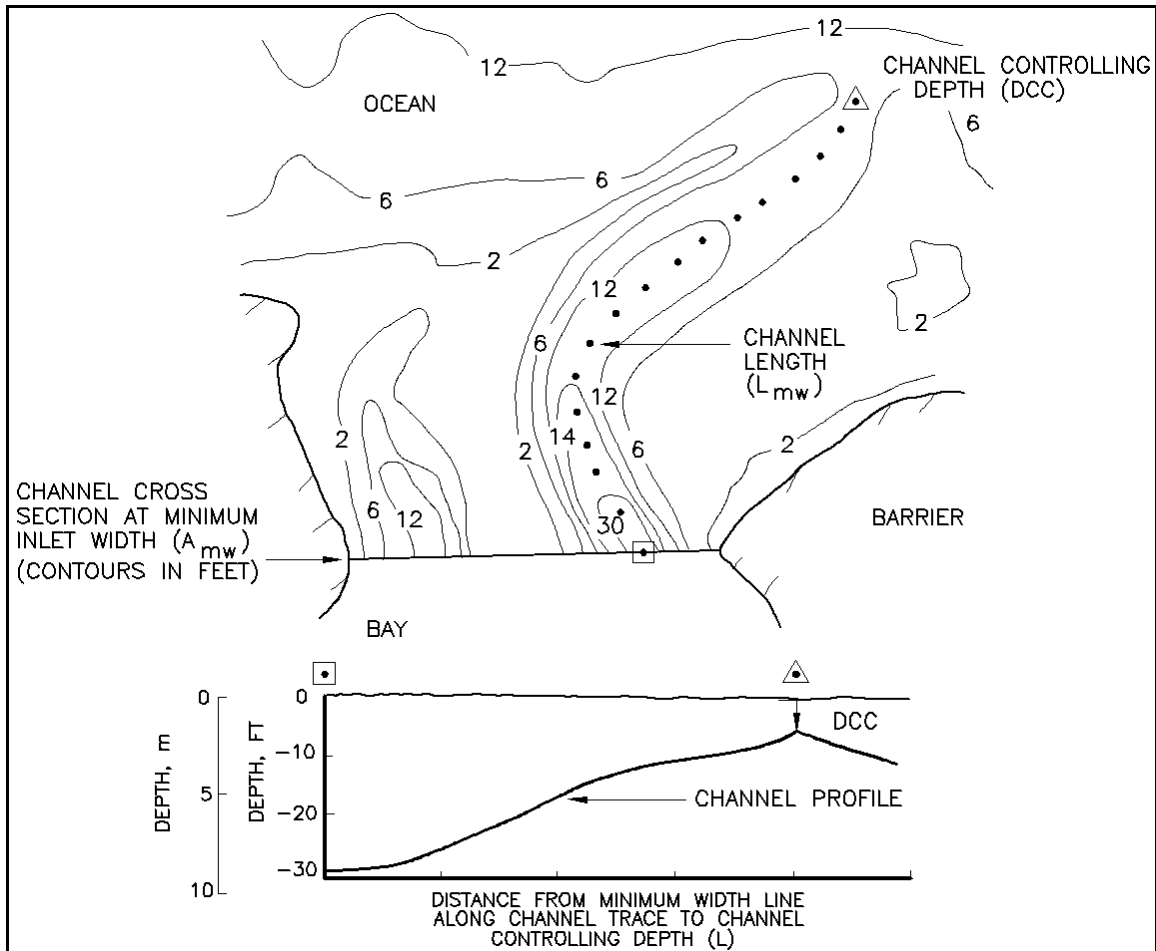


Figure II-6-3. Channel parameter measurement (Vincent and Corson 1980)

II-6-2. Inlet Hydrodynamics

a. Introduction.

(1) Many approaches are available to evaluate inlet hydrodynamics. Analytic expressions, numerical models, and physical models can be used. This section will present some simple analytic techniques to determine average velocities in a channel cross section due to the ocean tide and tidal elevation change in the bay. This section also will aid in understanding inlet response with regard to important parameters such as size of bay or channel area and length. Tidal inlet hydrodynamics are summarized by van de Kreeke (1988) and by Mehta and Joshi (1984).

(2) To characterize the development of inlet currents, COL E. I. Brown (1928) wrote the following:

To trace the characteristics of the flow of the tides through an inlet, assume the case of an inland bay being formed by the prolongation of a sandspit. It is quite evident that in the earlier stages of the growth of the spit the tide will rise and fall in the bay equally and simultaneously with its rise and fall in the surrounding ocean, and that a tidal current will be practically negligible. This state of affairs will continue for a long time, as long as the full and free propagation of the tidal wave is

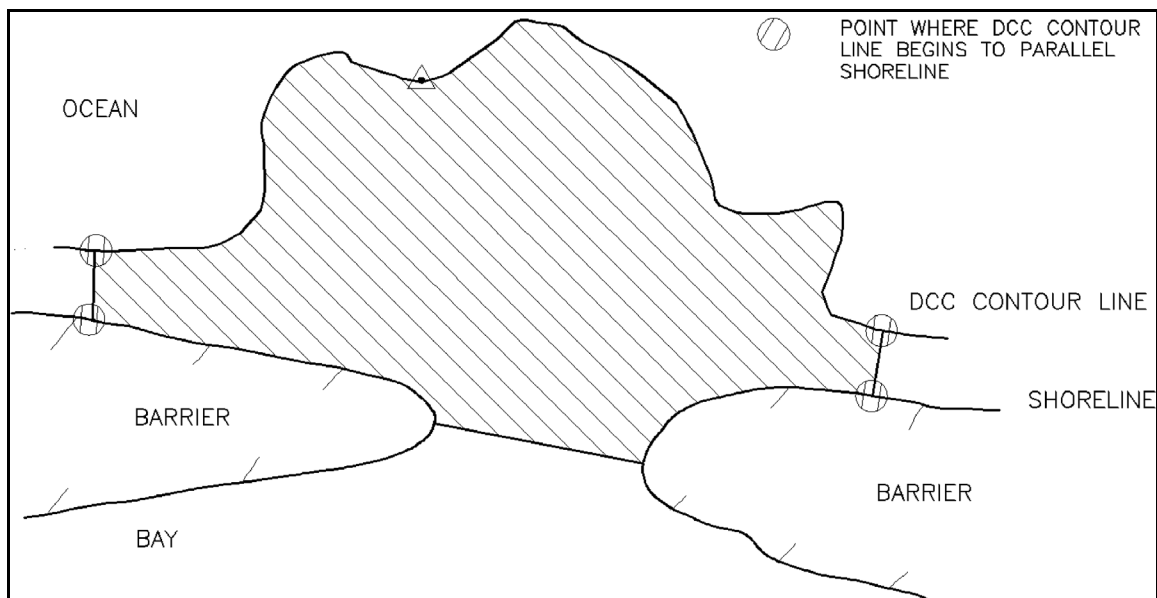


Figure II-6-4. Ebb delta area measurement (Vincent and Corson 1980)

unimpeded by the continually narrowing opening. When it does begin to be so impeded and the entrance acts as a barrier to the incoming tide, a delay in the advance of the tide will be caused, and a difference of head will occur between the water outside the inlet and that inside. This will create a hydraulic current into the bay, in addition to such movement as may be due solely to tidal wave propagation.

It is clear that as long as the inlet is wide and deep in proportion to the area of the bay, hydraulic currents will be small and tidal wave propagation will predominate. Tidal waves in the shallow waters near the shore will be essentially waves of translation, that is, the whole body of water moves with practically the same velocity horizontally. Now, if the size of the inlet becomes very small with respect to the bay area, tidal wave propagation will be negligible, the flow through the inlet will be hydraulic, that is, the water surface through the inlet will have a slope, causing a flow, and it can be considered mathematically in accordance with known hydraulic laws.

(3) With this in mind, early development of inlet hydraulics achieved reasonable results by using simplified approaches of steady-flow hydraulics to understand inlet currents and response of the bay (or lagoon) tide (Brown 1928). Keulegan (1951, 1967) solved the one-dimensional, depth-averaged shallow water wave equation for flow analytically. Others since have formulated a variety of analytical solutions for inlets (including van deKreeke (1967), Mota Oliveira (1970), Shemdin and Forney (1970), King (1974), Mehta and Özsöy (1978), Escoffier and Walton (1979), and DiLorenzo (1988)). Paralleling analytical development, physical models were used for detailed studies of inlet design (see below). More recently, numerical models have provided greater refinements and details using one-, two- and three-dimensional longwave equations of motion (including developments by Harris and Bodine (1977), Butler (1980), and Amein and Kraus (1991)). Some analytical models for inlets will be examined here to provide understanding of the inlet system and because they actually produce usable information with minimal effort. Application of the techniques of this chapter would include use of numerical models (e.g., Automated Coastal Engineering System (ACES); Leenknecht et al. 1992). ACES includes a spatially integrated one-dimensional numerical model. Additional information about ACES and other available models is provided in Part II-6-2, paragraph m, "Other methods for inlet analysis."

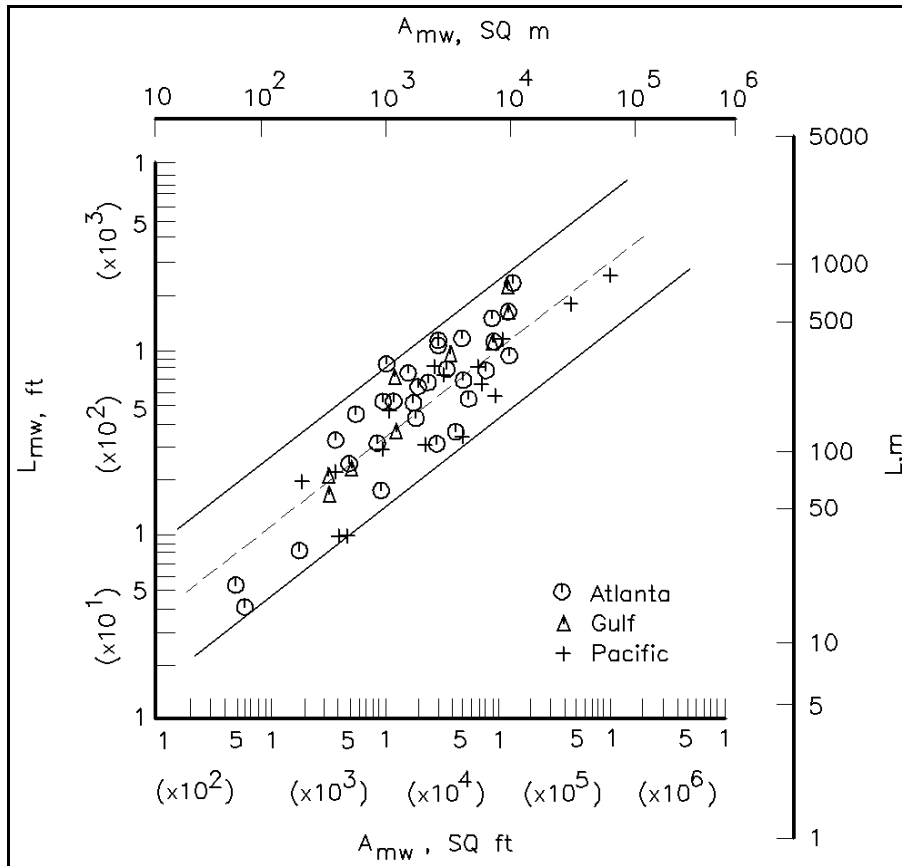


Figure II-6-5. Minimum width cross-sectional area of channel A_{mw} versus channel length L_{mw} (Vincent and Corson 1980)

b. Inlet currents and tidal elevations.

(1) A simple introduction to inlet hydraulics will consider applying the one-dimensional equation of motion and the continuity equation. We want to find the maximum inlet current, the tide range of the bay and the phase lag of the bay tide relative to the tide in the ocean in terms of parameters which can be easily measured or determined, including inlet cross-sectional area, bay surface area, ocean tide amplitude and period, length of channel, and head loss coefficients. The simplified inlet system is shown in Figure II-6-15. Keulegan's assumptions (1967) were as follows:

- (a) Walls of the bay are vertical.
- (b) There is no inflow from streams.
- (c) No density currents are present.
- (d) Tidal fluctuations are sinusoidal.
- (e) Bay water level rises uniformly.

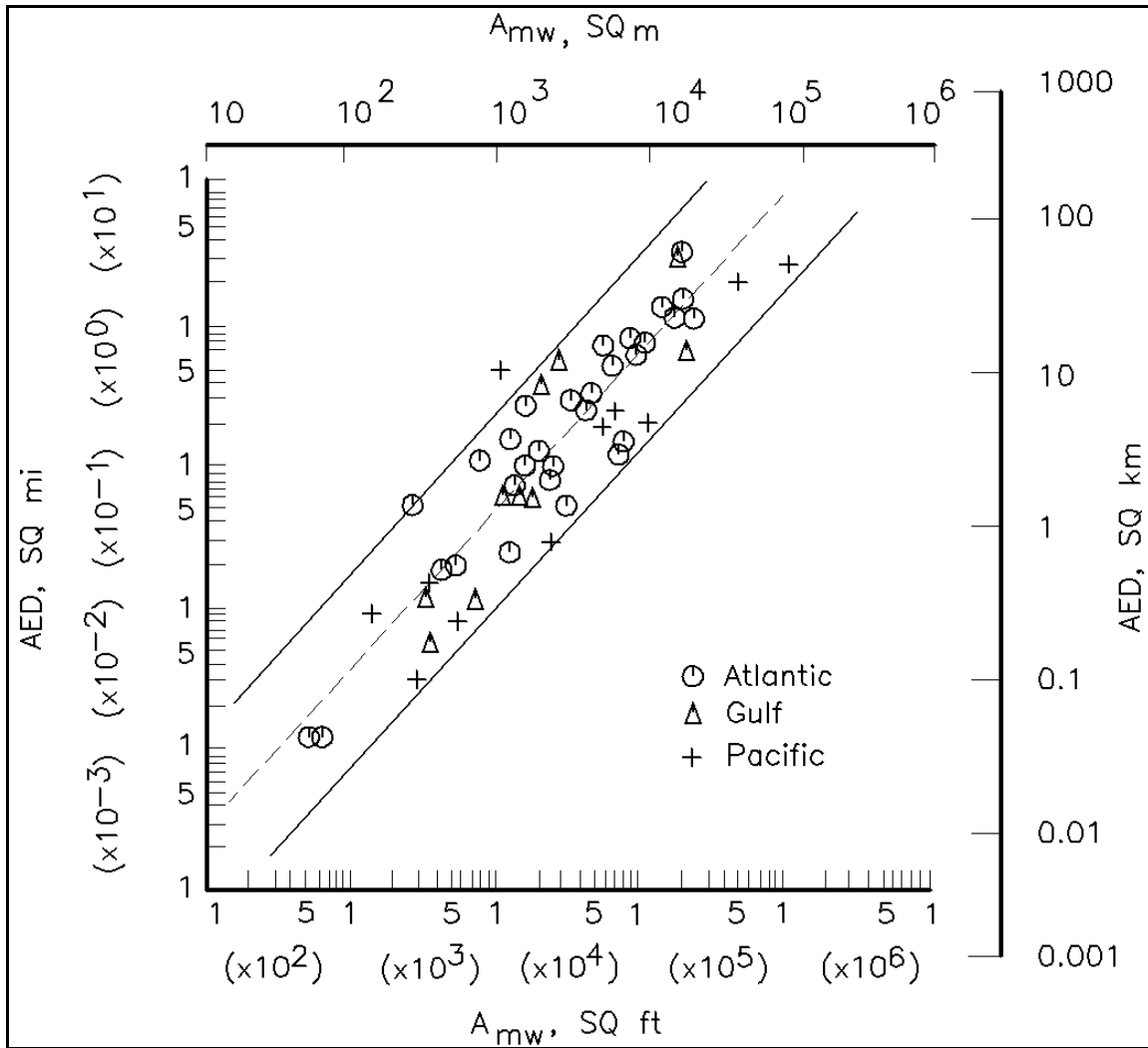


Figure II-6-6. A_{mw} versus ebb-tidal delta area (AED) (Vincent and Corson 1980)

- (f) Inlet channel flow area is constant.
- (g) Inertia of the mass of the water in the channel is negligible.

(2) Some assumptions may seem stringent (e.g., assumption (e), which essentially assumes a frictionless bay). This could be a problem if the entire bay is composed of very shallow tidal flats with no significant channelization. Also, in assumption (f), a relatively large tidal range compared to channel depth might occur. However, reasonable results can be determined for most cases. For more complex inlet systems, more sophisticated modeling should be performed, as discussed earlier.

(3) The one-dimensional equation of motion for flow in the channel is:

$$\frac{\partial V}{\partial t} + V \frac{\partial V}{\partial x} = -g \frac{\partial h}{\partial x} - \frac{f}{8R} V |V| \quad (\text{II-6-2})$$

where

V = average velocity in channel

h = channel water surface elevation

f = Darcy - Weisbach friction term

R = hydraulic radius

g = acceleration due to gravity

(4) Keulegan neglected local acceleration (the first term in Equation II-6-2) and integrated the equation over the length of the inlet. Using the equation of continuity for flow through the inlet into the bay:

$$VA_{avg} = A_b \frac{dh_b}{dt} \quad (\text{II-6-3})$$

where

A_{avg} = average area over the channel length

A_b = surface area of bay

dh_b/dt = change of bay elevation with time

(5) Combining Equations II-6-2 and II-6-3, Keulegan developed a solution for velocity and resulting bay tide which contained the dimensionless parameter K , known as the coefficient of repletion, or filling, which is defined as

$$K = \frac{TA_{avg}}{2\pi A_b} \sqrt{\frac{2g}{a_o \left[k_{en} + k_{ex} + \frac{fL}{4R} \right]}} \quad (\text{II-6-4})$$

where A_{avg} , A_b , g , f , and R are as defined above, and

T = tidal period

a_o = ocean tide amplitude (one-half the ocean tide range)

k_{en} = entrance energy loss coefficient

k_{ex} = exit energy loss coefficient

L = inlet length

R = inlet hydraulic radius (see Equation II-6-18)

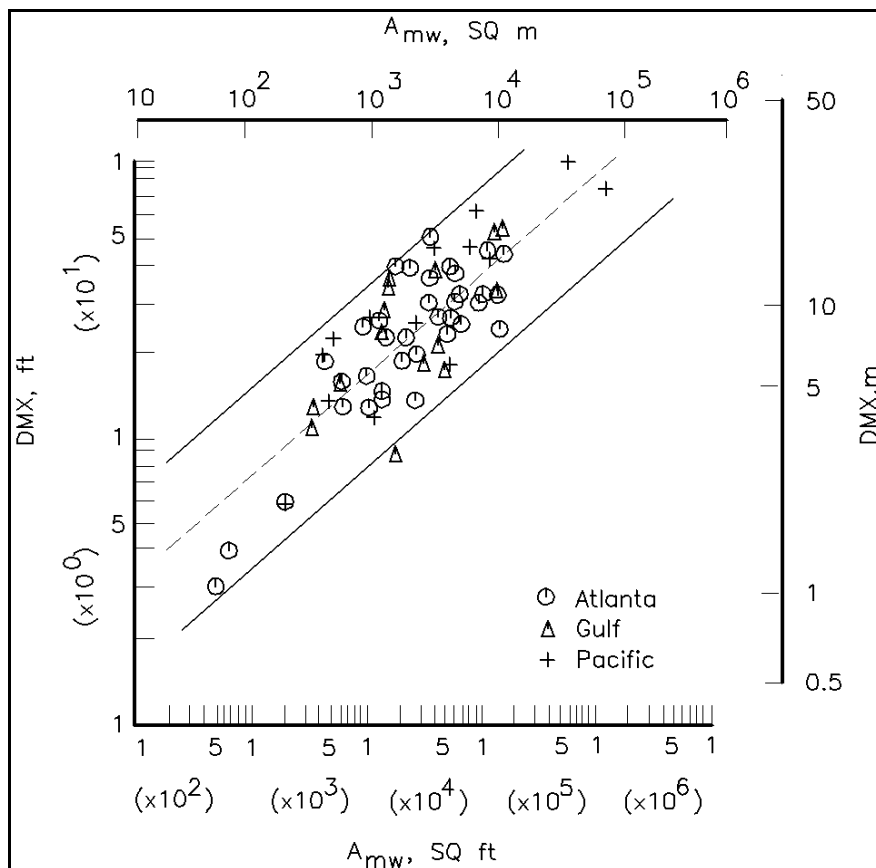


Figure II-6-7. A_{mw} versus maximum channel depth at minimum width section DMX (Vincent and Corson 1980)

(6) Keulegan's assumptions of prismatic channel cross section and vertical bay walls greatly simplify prototype conditions, because natural inlets generally have a complex morphology, making accurate determination of effective hydraulic radius, channel length, cross-sectional area, and bay area difficult. Considerable subjectivity is required to determine these values from bathymetric charts. Some aid is provided later in determining this information. Figure II-6-16 shows the variation of bay tide amplitude (a_b) to that of the ocean (a_o) and the phase lag (ϵ) for various values of the coefficient of filling K . Figure II-6-17 defines phase lag and provides a sample of output that can be determined from simple analytical models. Approximate values for k_{en} , k_{ex} , and f are given in Example Problem II-6-1. For flow entering an inlet channel, K_{en} is usually taken between 0.005 and 0.25. For natural inlets, which are rounded at the entrance, $K_{en} \approx 0.05$ or less. For inlets with jetties and flow bending sharply as it enters the inlet channel, $K_{en} = 0.25$ may be appropriate. The exit flow is usually taken near unity, meaning kinetic head is fully lost. If there is significant flow inertia, as in a very channelized bag, K_{ex} may be less than 1.0.

(7) King (1974) solved the same equations but included the effect of inertia (first term of Equation II-6-2). If inertia effect is important, then at times when the tide curves of ocean and bay intersect, there still would be a flow into the bay, e.g., on flood flow there would still be movement of the water mass into the bay, even as the bay elevation dropped below that of the ocean. This would be likely to occur when L is large (channel is long, and therefore a large mass of water moving through the inlet has significant inertia to move against an opposing head difference). Also the possibility exists that the inlet system could have a Helmholtz frequency (or pumping mode, where the basin oscillates uniformly) that is tuned to the forcing

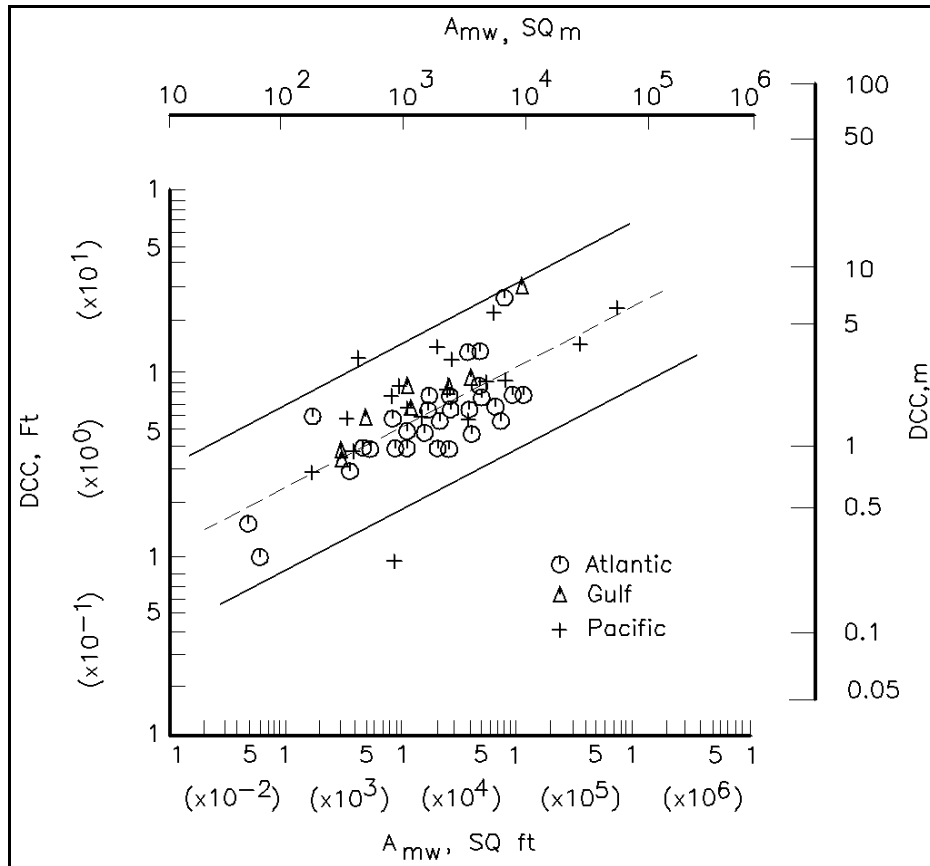


Figure II-6-8. A_{mw} versus minimum controlling channel depth DCC (Vincent and Corson 1980)

ocean tide and amplification of the bay tide could occur. This will be seen in King's solution also (and can be noted in Figure II-6-18 where the bay-ocean tide ratio is greater than one). King defines the dimensionless velocity as:

$$V'_m = \frac{A_{avg} T V_m}{2\pi a_o A_b} \quad (\text{II-6-5})$$

where V_m is the maximum cross-sectionally averaged velocity during a tidal cycle. (To determine V_m , use Equation II-6-5 and refer to Figure II-6-19.) Two parameters are calculated with the variables defined previously.

$$K_1 = \frac{a_o A_b F}{2 L A_{avg}} \quad (\text{II-6-6})$$

$$K_2 = \frac{2\pi}{T} \sqrt{\frac{L A_b}{g A_{avg}}} \quad (\text{II-6-7})$$

where F is defined as

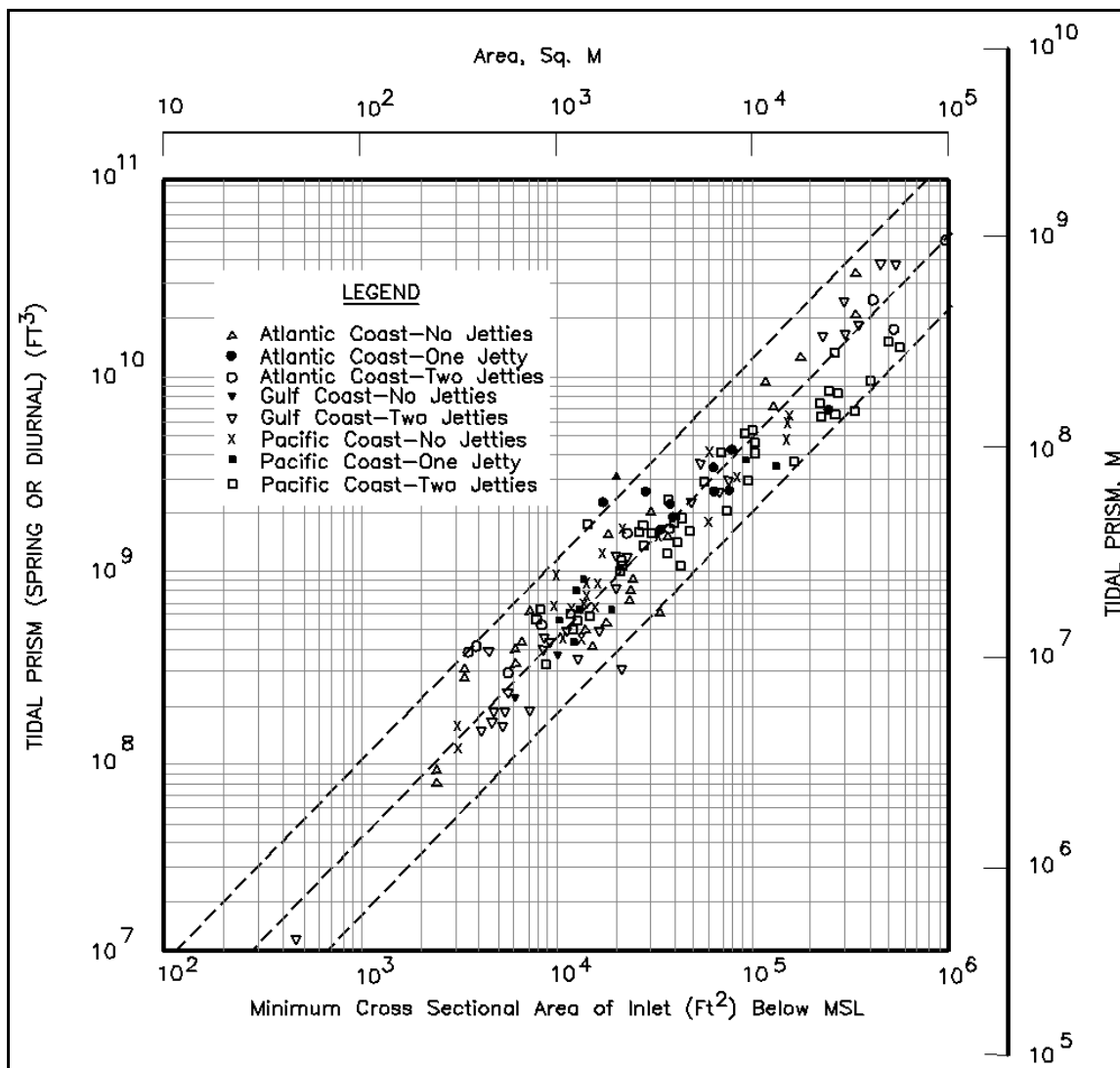


Figure II-6-9. Tidal prism-inlet area relationship

$$F = k_{en} + k_{ex} + \frac{fL}{4R} \quad (\text{II-6-8})$$

(8) Figures II-6-18 through II-6-20 provide a means to determine the bay tide range and phase and velocity in the channel. A sample problem is presented in Part II-6-2, paragraph *d*, where determining important parameters is discussed.

(9) Since channel resistance is nonlinear, channel velocity and bay tide will not be sinusoidal (Keulegan 1967). Other effects such as a relatively large tidal amplitude-to-depth ratio through the channel and nonvertical walls in the channel and bay may be important in causing nonsinusoidal bay tides (Boon and Byrne 1981, Speer and Aubrey 1985, Friedrichs and Aubrey 1988). However, for a first approximation, channel velocity over time is represented as

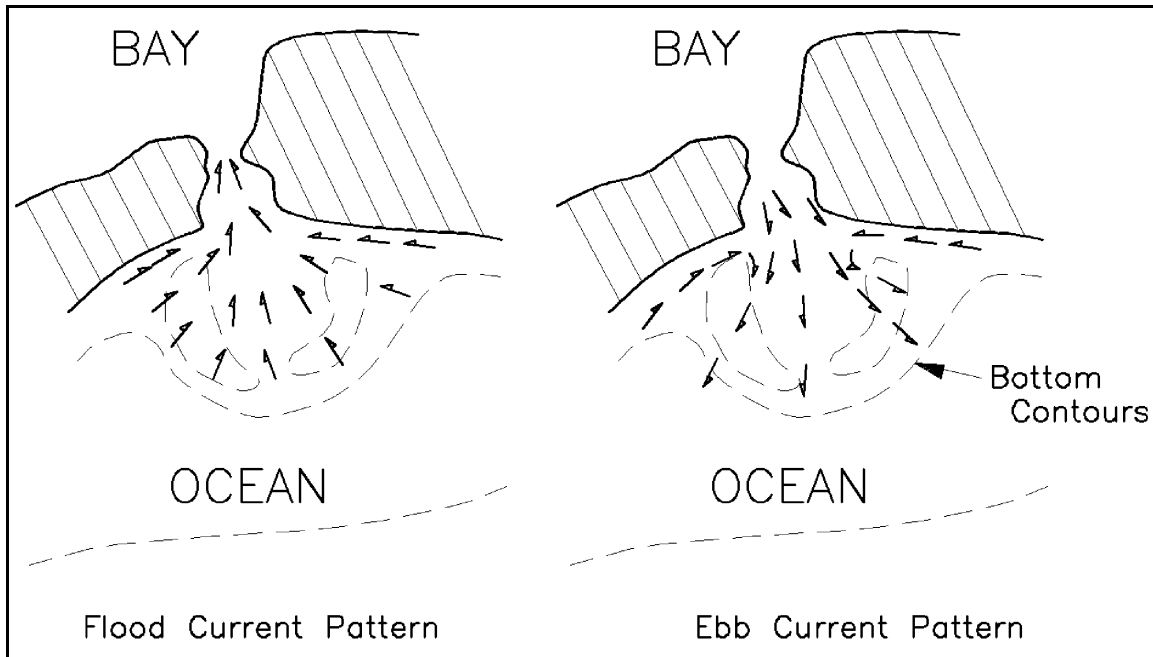


Figure II-6-10. Schematic diagram of flood and ebb currents outside an inlet (O'Brien 1969)

$$V \approx V_m \sin \frac{2\pi t}{T} \quad (\text{II-6-9})$$

and bay tide can be represented as (see Figure II-6-17)

$$h_b \approx a_b \cos \left(\frac{2\pi t}{T} - \varepsilon \right) \quad (\text{II-6-10})$$

where ε is phase lag, a_b is bay tide amplitude (one-half the bay tide range), T is tide period, and t is time of interest during the tide cycle. Also King's K_1 and K_2 are related to the Keulegan repletion coefficient K by

$$K = \frac{1}{K_2} \sqrt{\frac{1}{K_1}} \quad (\text{II-6-11})$$

c. Tidal prism.

(1) The volume of water that enters through the inlet channel during flood flow and then exits during ebb flow is known as the tidal prism. If the hydraulic analysis as described above is used, then tidal prism P can be calculated as

$$P = 2 a_b A_b \quad (\text{II-6-12})$$

(2) Another technique for prism estimation can use observed velocity (or discharge Q) data. Assuming a sinusoidal discharge in the channel and integrating over the flood or ebb portion of the tidal cycle

$$P = \frac{T Q_{\max}}{\pi} \equiv P = \frac{T V_m A_{\text{avg}}}{\pi} \quad (\text{II-6-13})$$

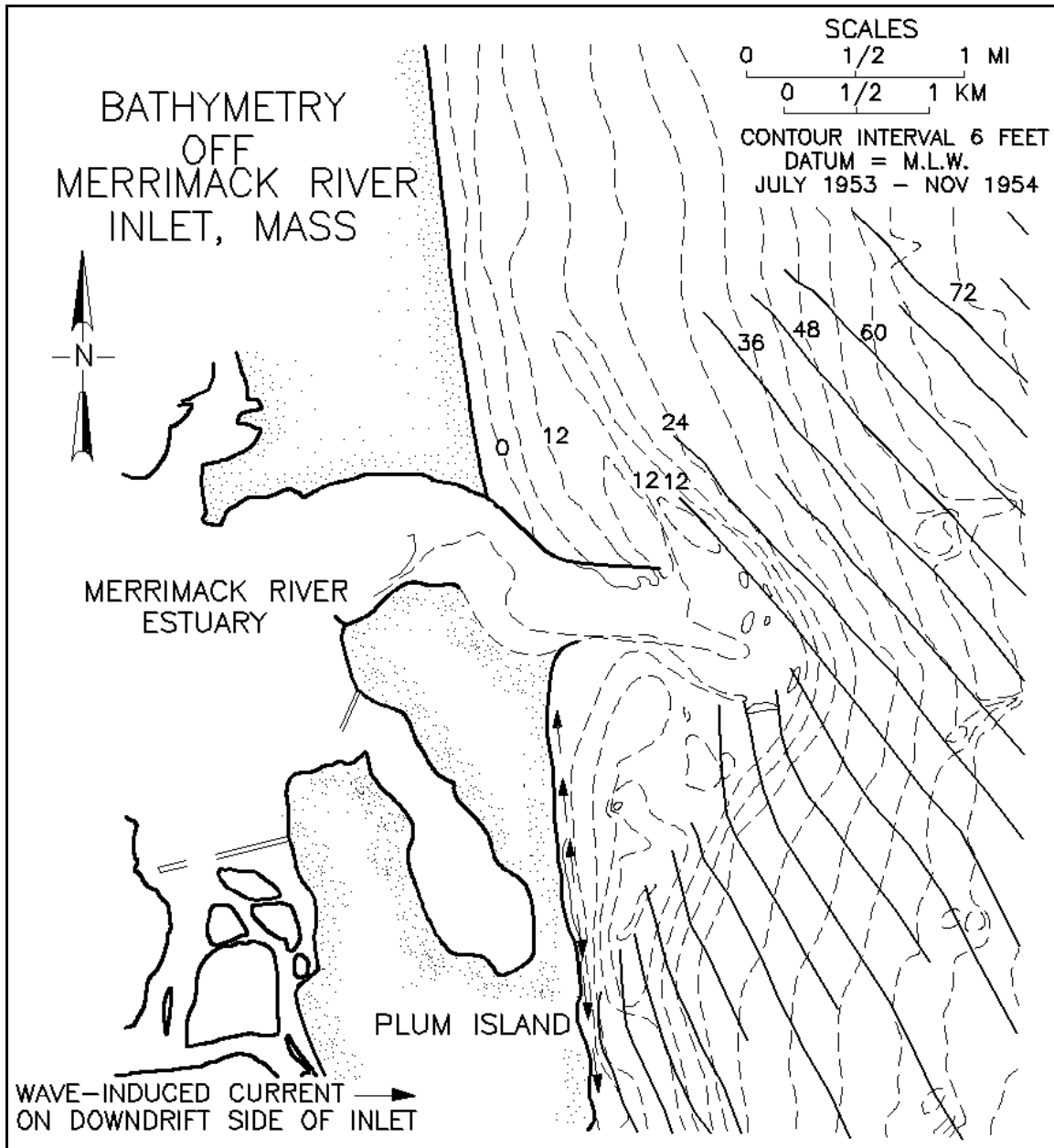


Figure II-6-11. Wave refraction pattern in the vicinity of the Merrimack River Estuary entrance, just south of the Merrimack Inlet (from Hayes (1971))

(3) To account for a non-sinusoidal character of the prototype flow, Keulegan determined

$$P = \frac{TQ_{\max}}{\pi C} \equiv P = \frac{TV_m A_{\text{avg}}}{\pi C} \quad (\text{II-6-14})$$

and found C varying between 0.81 and 1.0 for K , the filling coefficient, varying between 0.1 and 100. For practical application, if $0.1 < K < 1.8$, use $C = 0.86$, and for $K > 1.8$, use $C = 1.0$.